Morphofunctional Evidence of Changes in Principal and Mitochondria-Rich Cells in the Epidermis of the Frog *Rana* kl. *esculenta* Living in a Polluted Habitat

C. Fenoglio,[1] A. Grosso,[1] E. Boncompagni,[1] G. Milanesi,[1] C. Gandini,[2] S. Barni[1]

[1] Lab. Anatomia Comparata, Dipartimento di Biologia Animale, Università di Pavia, Piazza Botta 10, 27100 Pavia, Italy
[2] Dipartimento di Chimica Farmaceutica, Università di Pavia, Viale Taramelli 10, 27100 Pavia, Italy

Abstract. The epidermis of vertebrates is the body's principal barrier against environment and its possible contaminants. The presence of keratins, as well as specific detoxifying molecules or enzyme activities, in the various epidermis layers is believed to be involved in providing protection from harmful environmental influences. Anuran integument is poorly hornified and thus permeable to some endogenous and exogenous compounds and thus serves as a good bioindicator of overall environmental conditions. In the present investigation, we studied the epidermis of *Rana* kl. *esculenta* adult specimens collected at two different rice fields, relatively unpolluted and heavily polluted, respectively. Environmental pollution was assayed by chemical analysis performed on both sediments and animals. We evaluated the structural aspects of the epidermis at both light and electron microscopy levels and the pattern of keratinization by immunohistochemistry. Furthermore, we studied the activities of some enzymes (acid and alkaline phosphatase, nitric oxide synthase–related nicotinamide adenine dinucleotide phosphate dehydrogenase, glucose-6-phosphate dehydrogenase, catalase, nonspecific esterases, and succinic dehydrogenase) involved mainly in membrane transport, xenobiotics, and oxidative metabolism. Compared with controls, in polluted animals we found the following results: (1) an increase in pollutant levels (i.e., cadmium, mercury, and lead); (2) less keratinized superficial cells in the epidermis; and (3) changes in most enzyme activities in keratinocytes and mitochondria-rich cells (particularly glucose-6-phosphate dehydrogenase and esterases, both important to counteract oxidative and toxic stress). Taken as a whole, the present data indicate the morphofunctional plasticity of the frog epidermis in response to environmental contamination.

Anuran skin, which undergoes drastic structural changes during metamorphosis, exhibits a complex cellular composition and has several functions (*i.e.,* mechanical protection, ion and water transport, respiration, sensory perception). The general structure of the epidermis, including its cell types and keratin contents, differs in tadpoles and adults.

Larval epidermis is composed of three cell types: apical cells, skein cells (exclusive in tadpoles), and basal cells, which have been described in premetamorphosing larvae and are considered precursors of adult germinative cells (Fox 1986; Robinson and Heintzelman 1987; Izutsu *et al.* 1993). Skein cells are characterized by the presence of bundles of tonofilaments—the figures of Eberth—which morphologically express larval keratins (Ellison *et al.* 1985; Fox 1992; Spies 1997; Suzuki *et al.* 2001).

The stratified epidermis of adult anurans consists of several layers: germinative (or basal), spinous (or *spinosum*), granulous (or *granulosum*), and hornified (or *corneum*), all consisting of principal cells or keratinocytes showing a peculiar morphologic aspect depending on the layers (Fox 1986; Lindeman and Voute 1976). Flask-shaped mitochondria-rich cells (MRCs) are characteristic of anuran skin. They are intermingled in between keratinocytes and extend their necks into the interstice beneath the horny layer (Amstrup *et al.* 2001). They are variable in number in different species and in *Rana esculenta* they are more numerous in ventral than in dorsal skin (Ehrenfeld *et al.* 1976).

Within the epidermis, leukocytes, melanocytes, macrophages, and Merkel cells are also present. Compared with amniotes, anuran epidermis shows some structural differences; in particular, it exhibits a relatively thin hornified surface composed of one or two layers of flattened cells that retain their nuclei (see Alibardi 2003 for a review). Based on these structural traits, frogs can use the epidermis for respiratory gas (mainly carbon dioxide) and ion exchange. In fact, being exposed to both air and pond water, the skin of the frog represents one of the principal organs for body-fluid homeostasis. Several studies have suggested that in frogs, epidermal principal cells are mainly involved in active transport, whereas MRCs are specialized in proton and bicarbonate secretion (Lindeman and Voute l976; Fox 1986; Ehrenfeld and Klein 1997).

Hence, numerous investigations on frog skin have focused mainly on morphologic and ion-transport changes under both natural and experimental conditions (i.e., seasonality or different ion concentration) (Barni *et al.* 1987; De Piceis Polver *et al.* 1988; Vanatta and Frazier 1989; Malvin and

Hlastala 1989) and in relation to environmental contamination as well (Ferrari and Salibian 1999; Suwalsky *et al.* 2000, 2001, 2004). To our knowledge, however, only Johnson *et al.* (2000) have undertaken studies to date on the detoxifying and antioxidant responses of the amphibian epidermis to counteract effects of contaminants. Instead, some researchers have focused attention on the study of the antioxidant defense mechanisms of mammal skin after exposure to oxidative stressors, including chemical pollutants and ionizing, ultraviolet, and UV irradiation (see Kohen [1999] for a review).

It is worthy of note that a variety of industrial, agricultural, and urban chemicals can contaminate water bodies, such as rice fields, inhabited by amphibians. In a previous study, we investigated the presence of contaminants in *R. esculenta* tadpoles collected at two different rice fields, one relatively unpolluted and the other heavily polluted. In the latter, the occurrence of several contaminants was significantly greater compared with the former. Moreover, we observed morphofunctional changes in the livers of polluted adult frogs collected in the same rice fields, which indicate an adaptive response of this organ—through both enzymatic and nonenzymatic mechanisms—to counteract environmental pollution (Fenoglio *et al.* 2005).

Although liver activity is of primary importance in xenobiotic biotransformation processes, the integument is the first organ system that interacts with environmental constituents (i.e., air, water, soil sediment). Thus, perturbations of the amphibian epidermis could be induced by exposure to pollutants.

We therefore studied the epidermis of adult green frogs (*R. klepton esculenta*) collected in both control and relatively polluted rice fields with the aim of obtaining additional information on the ability of the frogs' component cells to respond to environmental pollution. Both rice-field sediments and animals were submitted to chemical analysis to assess environmental contamination. In all of the animals, we analyzed the morphologic structure of the ventral skin using both light and electron microscopy, including keratin immunolocalization trials.

We also studied some enzyme activities as indicators of oxidoreductive metabolism (glucose-6-phosphate dehydrogenase [G6PDH], succinic dehydrogenase [SDH], nitrous oxide synthase [NOS]–related nicotinamide adenine dinucleotide phosphate [NADPH] dehydrogenase [NOS/NADPHd]) antioxidant and defense functions (catalase [CAT], acid phosphatase [AcPase], and α-naphtyl acetate and butyrate esterases [ANAE and ANBE]) and transport activity (alkaline phosphatase [AlkPase]) The presence of reactive oxygen species (ROS) was also investigated.

Materials and Methods

Animals and Study Sites

Adult frogs (*R. kl. esculenta*) of both sexes were collected in two rice fields: the control site, which was flooded with relatively unpolluted resurgence water (site 1), and the tested site flooded with the heavily polluted waters of the River Lambro (site 2). Sediment samples were also collected at the same sites using a 30-cm depth core. Because the Lambro collects industrial and human waste from densely inhabited

areas, its waters host a variety of persistent contaminants, heavy metals, and organic micropollutants (Marchetti 1991). Moreover, they are characterized by high values of biochemical (BOD) and chemical oxygen demand (COD) along with phosphate and nitrite and ammoniac nitrogen with higher concentrations of chromium, nikel, manganese, and aluminum than those permitted by the environmental regulations of the Regione Lombardia (unpublished data, Azienda Ricerca Consulenza Ambientali, Lodi, 1996 to 2001).

The analysis of the biological quality and chemicophysical features of the Lambro River is performed by the Agenzia di Ricerche e Consulenze Ambientali of Cameri (NO) every 5 years. Compared with those of the preceding years, however, the latest samplings showed a diminishing degree of water pollution.

Chemical Analysis

Whole adult green frogs and sediments from the two sites were submitted to chemical analysis to test differences in water pollution in the two areas. Previous chemical analysis in the same areas had been conducted on tadpoles of *R. esculenta* (Fenoglio *et al.* 2005). The homogenized animal samples (control-CL, contaminated frogs-CT) and sediments were analyzed using adsorption spectrophotometry (AAS) for cadmium, chromium, mercury, and lead and high-resolution chromatography according to Mateo *et al.* (1999) for the following organochlorine compounds: hexachlorobenzene (HCB); hexachlorocyclohexane α, β, and γ (lindane) isomers (HCHs); heptachlor epoxide and α-endosulfan (cyclodienes); *p,p*'-DDT, *p,p*'-DDE, *p,p*'-DDD, and *o,p*'-DDT (DDTs); and polychlorinated biphenyls (PCBs). The same procedure was used for sediment samples.

AAS. Cadmium, chromium, and lead were analyzed by a Perkin-Elmer Analyst 600 AA spectrophotometer. Mercury was analyzed by a Perkin-Elmer FIAS-100 and by a Perkin-Elmer 3110 AA spectrophotometer (Perkin Elmer Italia SpA, Monta-Mi, Italia). Instrument control and data calculation were performed on personal computer using AA WinLab software. To eliminate organic matter, the samples were mineralized without previous washing using a CEM-MDS 81D microwave oven (LEM Corporation, Matthews, NC), then dissolved in 30% nitric acid as described by Fasola *et al.* (1998). The materialization technique was tested for element recovery on reference material. The tests for cadmium, chromium, mercury, and lead gave recoveries ranging from 98% to 101%. Preliminary tests were carried out using standard solutions of pure single element dissolved in nitric acid and water (30% v/v) at three concentrations. The calibration curves were found linear for the following ranges as absolute concentrations—cadmium-2-4-6 ppb; chromium-5-10-20 ppb; mercury-2-4-8 ppb; lead-3-6-12 ppb—corresponding to the detection limit on the biological sample of 0.020 ppm for chromium, 0.030 ppm for cadmium, 0.010 ppm for mercury, and 0.030 ppm for Pb. Estimates were made according to standard addition methods (Baden 1980) supported by PC Software.

High-resolution chromatography. Organochlorine analyses were carried out by high-resolution gas chromatography on a Perkin-Elmer AutoSystem (Perkin Elmer Italia SpA, Monta-Mi, Italia) equipped with a 30-m fused silica capillary column of 0.53-mm ID (BPX5 from SGE, Ringwood, Australia) coupled to an electron-capture detector (ECD). Chromatographic conditions were optimized for the separation of the compounds under study at a suitable analysis time. The oven was programmed from the initial temperature of 145°C to 276°C at a rate of 2.5°C/min, with injector (Jade septum-less) temperature of 290°C and of 310°C, and with carrier gas (He) at a linear velocity of 25 cm/s. Chlorinated compounds were localized using PCB Nos. 1

and 209 (standards added to samples from the beginning) employing the Situation Units System for identifying peaks in the chromatograms (Mateo *et al.* 1998). High-resolution chromatographic analysis and quantification of organochlorine (OC) residues followed the corrected Ballschmiter and Zell nomenclature system for PCBs (Guitart *et al.* 1993). Aroclor 1254 was used to quantify PCBs. The total PCB concentration (ΣPCBs) was calculated as the sum of individual congener concentrations. Recoveries of selected pesticides (DDTs and HCHs 71% to 100%, *n* = 5) and PCBs (77% to 100%, *n* = 4) were calculated and considered satisfactory, but no corrections were made based on recoveries. Because cyclodienes are partially degraded by the acid attack, their values should be considered as underestimated. Blanks were processed between samples to check for the absence of external contamination. Detection limits for the different compounds were as follows: HCBs = 3 ppb; HCHs = 1 ppb; heptachlorepoxide and α-endosulfan = 1 ppb; *p,p*'-DDE and *o,p*'-DDT = 2 ppb; *p,p*'-DDD and *p,p*'-DDT = 3 ppb; and ΣPCBs = 25 ppb.

Morphologic and Histochemical Analyses

Tissue processing and histochemical staining. The animals from both areas were used within 1 day of arrival in the laboratory. At least six specimens of adult frogs were used. They were deeply anesthetized with a buffered solution of MS-222 (in accordance with Guide for the Care and Use of Laboratory Animals) and then killed by decapitation. The ventral skin was removed, cut into small pieces (1 × 2 mm), and processed for either light or electron microscope procedures.

For electron microscopy studies, fragments of skin were fixed by immersion for 3 hours in ice-cold 1.5% glutaraldehyde (Polysciences, Warrington, PA), 0.05 M cacodylate buffer at pH 7.4, containing 7% sucrose, and postfixed with 1% OsO_4 (Sigma Chemical, St. Louis, MO) in the same buffer for 2 hours at 4°C. Samples were dehydrated in graded series of ethanol and embedded in Epon 812. Ultrathin sections, 600 Å, obtained with a C. Reichert OMU3 ultramicrotome (Reichert, Vienna, Austria), were contrasted with uranyl acetate and Reynold's lead citrate solution. The specimens were then observed in a Zeiss EM 300 electron microscope (Carl Zeiss SpA, Italia)

For morphologic and immunohistochemical light microscopy analysis, ventral skin pieces were fixed in 2% paraformaldehyde in 0.1 M phosphate buffer at pH 7.4 for 24 hours and processed routinely until they were embedded in Paraplast wax. Some small pieces of frog skin were frozen in liquid nitrogen and stored at −80°C for histochemical detection of some enzyme activities and ROS expression.

The relative expression levels of immunodeposits and the enzyme reaction product of different specimens were evaluated by two independent observers. Values of positivity were scored as weak (+), moderate (++), and intense (+++), respectively. Sections lacking reactivity were graded as negative (−).

Sections examined for their morphologic detail stained with either hematoxylin-eosin (H&E) or toluidine blue. Sections obtained from Paraplast-embedded samples, 6-μm thick, underwent the following histochemical reactions: (1) terminal deoxynucleotidyl-transferase (TUNEL) assay to detect apoptotic cell death; (2) Periodic Acid Schiff (PAS) reaction (with and without previous digestion with 0.2% α-amylase) for neutral glycoproteins; and (3) Alcian blue (AB) at pH 1-PAS and AB at pH 2.5-PAS reaction.

For TUNEL labelling, the ApopTag Peroxidase Kit (CHEMICON International) was used according to the detail protocol supplied with the kit. The skin sections were processed for TUNEL reaction, revealed with diamino benzidine (DAB), and counterstained with hematoxylin. As negative control the terminal deoxynucleotidyl-

transferase incubation was omitted; no staining was observed under these conditions. Staining procedures of PAS and AB/PAS were conducted according to Pearse (1972) to identify carboxylated acid, sulfated acid, and neutral complex carbohydrated.

Immunohistochemistry. In previous immunohistochemical studies on several species of amphibians (Spies 1997; Alibardi 2001, 2002), antibodies against mammalian keratins were successfully employed. Moreover, molecular studies support immunohistochemistry as a successful indicator that both amphibian type I and type II keratins show a structural homology with human keratins (Fuchs and Marchuk 1983; Hoffman and Franz 1984; Hoffman *et al.* 1985).

In the present study for keratin immunolocalization, the following monoclonal antihuman keratin antibodies were applied: (1) AE1 (Serotec), which recognizes most acidic type I keratins (40 to 58 kDa); (2) AE2 (Acris), which recognizes some acidic and basic keratins (56 to 68 kDa); and (3) AE3 (Serotec), which recognizes most basic type II keratins (58 to 67 kDa).

Sections obtained from Paraplast-embedded samples, 6-μm thick, were deparaffinized and hydrated. Afterward, they were submitted to a protein digestion with trypsin 250 for 10 minutes, and then they were treated with 3% H_2O_2 in 10% methanol for 20 minutes to block endogenous peroxidase activity. After washing in 0.01 M phosphate-buffered saline (PBS) rinse, the sections were incubated with the primary antibody at an appropriate dilution (1:100 for AE1 and AE3 and 1:20 for AE2) at room temperature for 3 hours. After brief rinsing with PBS, the peroxidase-conjugated EnVision[+] System HRP, which is based on an HRP-labelled polymer and conjugated with the secondary goat antimouse antibody (Dako), was applied to the sections for 1 hour at room temperature. The chromogen DAB was used to visualize the secondary antibody. The sections were dehydrated and mounted with Entellan. The specificity of the immunoreactions was controlled by replacing the primary antisera with the dilution buffer; no staining was observed under these conditions. Antibodies against AE1, AE2, and AE3 keratins were also tested on normal human skin samples as biological control.

Enzyme histochemistry and ROS demonstration. Sections 6-μm thick were obtained from frozen samples with a Leica CM 1850 cryostat, mounted on glass slides coated with poly-L-lysine, and stored at −25°C until used. The activity of the following enzymes was demonstrated by using their respective incubation media: AcPase (EC 3.1.3.2) according to Burstone (1962); 0.1 M acetate buffer (pH 5); 0.4 mM naphthol AS-Bl phosphate dissolved in N,N-dimethylformamide; Fast Red Violet LB 0.5 mg/1ml of final solution (incubation for 40 minutes 37°C); AlkPase (EC 3.1.3.1) according to McGadey (1970) as modified by Van Noorden and Jonges (1987); 0.1 M Tris-HCl buffer (pH 9) containing 15% polyvinyl alcohol (PVA), 0.7 mM 5-bromo-4-chloro-3-indolylphosphate, 0.32 mM 1-methoxyphenazine methosulfate; 5 mM $MgCl_2$, 5 mM sodium azide, 5 mM tetranitro BT (TNBT) (incubation for 7 minutes at 37°C); NOS/NADPHd (EC 1.6.99.2) on prefixed sections in 4% paraformaldehyde (buffered with 0.1 M phosphate at pH 7.4) for 15 minutes at 4°C according to Nakos and Gossrau (1994) with our modifications (Fenoglio *et al.* 1997); 15% PVA, 0.1 M phosphate buffer (pH 7.4), 5 mM levamisole, 2 mM NADPH, 3 mM NBT, 0.2% Triton X, 0.2% paraformaldehyde (incubation for 50 minutes at 37°C in the dark); G6PDH (EC 1.1.1.49) according to Van Noorden and Frederiks (1992); 0.1 mM phosphate buffer (pH 7.4) containing 15% PVA, 10 mM glucose-6-phosphate, 0.8 mM $NADP^+$, 0.32 mM 1-methoxyphenazine methosulfate, 5 mM $MgCl_2$, 5 mM sodium azide, 5 mM TNBT (incubation for 3 minutes at 37°C); CAT (EC 1.11.1.6) according to Van Noorden and Frederiks (1992); 0.1 mM glycine-NaOH buffer (pH 10.5) containing 2% PVA, 5 mM DAB, 18 mM H_2O_2 (incubation for 30 minutes at 37°C); SDH (EC 1.3.99.1) according to Loyda *et al.* (1979); 0.1 M phosphate

Table 1. Concentration of cadmium, chromium, mercury, lead, and some organic compounds in sediments[a]

Area type	Cadmium	Chromium	Mercury	Lead	H	HE	Endosulfan
Unpolluted area							
No. (%)	5 (100)	5 (100)	5 (100)	5 (100)	5 (0)	5 (80)	5 (20)
Mean	0.1	58.61	0.06	0.54	ND	0.015	0.03
Min/max	0.047/0.13	55.98/61	0.03/0.13	0.05/1.004		0.007/0.2	ND/0.05
Polluted area							
No. (%)	6 (100)	6 (100)	6 (100)	6 (100)	6 (50)	6 (83)	6 (100)
Mean	0.76	55.53	1.46	7.16	0.09	0.06	0.82
Min/max	0.28/1.07	42.5/60.9	0.30/3.01	5.97/8.07	ND/0.16	0.004/0.12	0.09/2.01
Difference among study areas ($p =$)	0.002	NS	0.015	0.001			

[a] The values are No. of sample (percentage frequency of samples with concentrations higher than above the detection limits), arithmetic mean, maximum and minimum values, ppm dry weight for heavy metal and ppb dry weight for organic compounds.

H = Heptachlor.

He = Heptachlor epoxide.

NS = Not significant.

buffer (pH 7.4), 50 mM sodium succinate, 0.32 mM phenazine methosulfate, 5 mM sodium azide, 2.5 mM TNBT (incubation for 5 minutes 37°C); ANAE, (EC 3.1.1.1) according to Castell-Rodriguez *et al*. (2001); 10 ml 0.1 M phosphate buffer (pH 7.4) containing 600 µl hexazotized Pararosaniline and 1.2 mg α-naphtyl acetate in 500 µl acetone (incubation for 30 minutes at room temperature); ANBE (EC 3.1.1.2) according to Higgy *et al*. (1977); 10 ml 0.1 M phosphate buffer (pH 8.0) containing 10 µl α-naphtyl butyrate in 500 µl acetone, and 15 mg Fast Blue BB salt (incubation for 30 minutes at room temperature).

All media were freshly prepared just before incubation. After incubation, tissue sections were rinsed in incubation buffer and in distilled water to stop reaction and then mounted in glycerol jelly. We compared the relative intensities of enzyme reactions among control and polluted samples on the same slide to avoid possible discrepancies resulting from different processing times.

The specificity of each enzymatic reaction was tested by submitting frog skin sections in incubation media without substrate. Incubation of the slices in a complete medium with 10 mM sodium fluoride, inhibitor of AcPase, and nonspecific esterases was used to prove the specificity of these reactions. For AlkPase, samples were also incubated in presence of 10 mM levamisole, its specific inhibitor. For NOS/NADPHd, fixed sections were alternatively incubated in a medium containing NADH instead of NADPH. No reaction products were detected in any of the control sections.

To detect ROS, fresh cryostat sections were incubated in a medium, prepared according to Kerver *et al*. (1997), containing 12.5 mM DAB, 5 mM $MnCl_2$, and 40 mM $CoCl_2$ dissolved in 10% PVA in 100 mM Tris-maleate buffer (pH 8.0) at 37°C. After an incubation period of 30 minutes, the sections were rinsed in hot distilled water to stop reaction and to remove the viscous incubation medium. The slides were then mounted in glycerol jelly, observed, and photographed immediately afterward with a light microscope.

The chemicals used for histochemical reactions were purchased from Sigma Chemical except for sodium azide, which was purchased from E. Merck (Darmstadt, FRG), and magnesium chloride, manganese chloride, and cobalt chloride, which were purchased from Carlo Erba (Milan, Italy).

Results

Chemical Analysis

The results of sediment and tissue analyses from the two sites confirmed the higher state of contamination at site 2 compared with site 1. Contamination levels in the sediments collected in the two study areas are shown in Table 1. Cadmium, mercury, and lead were present in a significantly higher concentration in samples from the polluted area. Heptachlor was not detected in the control area, whereas it was present in 50% of samples from the polluted site. Heptachlor epoxide percentage was similar in the two sites. Endosulfan was present in a higher percentage of samples from the polluted site.

Pollutant levels in adult frogs collected at the two study areas are shown in Table 2. There were significant differences in cadmium, mercury, and lead concentrations between the samples collected in the two different locations. Heptachlor was not detected in any samples from either area. Heptachlor epoxide percentage was higher in samples from the polluted area. Endosulfan was also present in a higher percentage of samples from the polluted site. In general, contaminant concentrations in tissue, except for chromium, reflected those of the metals in the sediments.

Morphology and Histochemistry

At light microscopy, control frog epidermis was found to consist of four to seven layers of keratinocytes with a superficial flat layer of hornified cells showing picnotic nuclei. A thin interstice was present between the external horny layer and the epidermal layer just below. Cells in the deeper layers (basal to granulous) displayed more abundant cytoplasm and spheroid or oval nuclei.

Generally, in the skin sections of frogs collected in the polluted area, no degenerative alterations were detected. However, at light microscopy the granulous and corneus layers of the epidermis displayed a tendency to become thicker. In addition, the presence of some pale keratinocytes was noticed in the subcorneal layer.

Ultrastructural observations showed different features of the keratinocytes. In basal cells, the cytoplasm was abundant and contained a few organelles, such as endoplasmic reticulum, ribosomes, and keratin filaments arranged in bundled tonofilaments, whereas spinous and granulous layer cells contained an increasing number of small and dense mucous granules as well as thickly bundled tonofilaments according to a base–surface gradient (Fig. 1a). Pale cells containing numerous

Table 2. Concentration (average ppm dry weight) of the heavy metals and (average ppb dry weight) some organic compounds in adults from the two study areas[a]

Area	Cadmium	Chromium	Mercury	Lead	H	HE	endosulfan
Control area							
No. (%)	4 (100)	4 (100)	4 (100)	4 (100)	5 (0)	5 (40)	5 (60)
Mean	0.05	4.41	0.04	0.64	ND	0.09	0.05
Min/max	0.01/0.07	3.87/4.72	0.02/0.06	0.48/0.82		ND/0.44	ND/0.12
River Lambro							
No. (%)	4 (100)	4 (100)	4 (100)	4 (100)	4 (0)	4 (100)	4 (100)
Mean	0.76	7.05	0.68	2.25	ND	0.23	0.08
Min/max	0.33/1.26	3.61/8.59	0.13/0.92	0.66/3.55		0.03/0.42	0.01/0.14
Difference among study areas ($p =$)	0.011	NS	0.014	0.049			

[a] Each sample was made by 5 individuals collected at various sites within a study area.
H = Heptachlor.
He = Heptachlor epoxide.
NS = Not significant.

mitochondria, *i.e.*, MRC, along with some tonofilaments were dispersed among the keratinocytes.

Compared with control specimens, the epidermis ultrastructure of most polluted animals showed some differences. In the latter, the cytoplasm of granulous layer cells contained numerous granules, lysosomes, tonofilaments, and a large number of vesicles, often associated with ribosomes, having amorphous material inside (Fig. 1b). In most samples, the subcorneal spaces appeared dilated and contained amorphous material forming dense deposits (Figs. 1c and 1d). Moreover, in several samples the superficial cells of the horny layer often appeared thicker and cytoplasm showed pale amorphous zones inside (Figs. 1d and 1e). MRCs were generally similar to those observed in controls (Fig. 1b).

Generally, after the *in situ* analysis of DNA fragmentation by TUNEL method, positive reaction was rare in epidermal cells. However, in polluted samples, cells positive for TUNEL were sometimes more numerous than in controls (Figs. 2a and 2b). They were localized mainly in basal and intermediate layers.

In control samples, light to moderate PAS positivity was detected in basal and intermediate cell layers, respectively. In polluted animals, intense and almost homogeneous PAS staining was observed in all layers, and a dense rim of PAS-positive amorphous material was detected in the subcorneal space (Figs. 3a and 3b).

After AB staining at pH 2.5, the epidermal cells of both control and polluted animals displayed negligible positive responses. After AB reaction at pH 1, most principal cells in polluted specimens showed increased responses from basal to granulous layers compared with controls (data not shown). A positive rim was detected resting on the horny layer of all of the samples submitted to AB staining.

Immunohistochemistry

Immunostaining by the AE1 antibody (to label acidic keratins) resulted in moderate positive responses of the epidermal basal layer in both groups of samples. Moreover, MRCs were stained by AE1 antibody strongly in the control group and moderately in the polluted one. In addition, the horny layer was weakly stained in the last sample group (Figs. 3c and 3d). Secretory cells in mucous glands also revealed strong immunoreactivity (Figs. 3c and 3d).

The use of AE2 antibodies to label both acidic and basic keratins with high molecular weight allowed selective and intense staining of the horny layer in control epidermis. In contrast, immunoreactivity was low in the same layer of the polluted samples. No reactivity was detected in MRCs of both groups (Figs. 3e and 3f).

In control animals, the AE3 antibody (used to label basic keratins) predominantly stained the epidermal superficial layers, whereas in polluted samples the labelling was light and diffused throughout the strata. However, immunostaing responses were stronger in controls than in polluted animals (data not shown). The results collected from immunohistochemical staining trials of cytokeratins are summarized in Table 3.

Enzyme Histochemistry

The AcPase reaction labelled the upper cytoplasm regions in the cell of the intermediate layers, including cells beneath the horny coat; a moderate enzymatic activity was observed in control frogs, whereas the positivity of the reaction product ranged from intense to strong in most polluted samples (Figs. 4a and 4b).

Control frog epidermis displayed strong AlkPase activity, which increased from the upper-intermediated to the outer layers, but the horny coat gave no response. A similar staining pattern was detected in polluted samples, but they showed light to moderate reactivity patterns (Figs. 4c and 4d).

NOS/NADPHd activity was detected in both keratinocytes and MRCs, with an increased expression in polluted skin samples compared with controls. In both cell types, the reaction product was mainly observed in the upper pole of the cells (Figs. 4e and 4f).

G6PDH activity was moderately expressed in all epidermal cells of control samples except for those in the layer beneath the horny coat (Fig. 5a). Compared with controls, stronger responses were observed in the intermediate epidermal layers of polluted frogs (Fig. 5b).
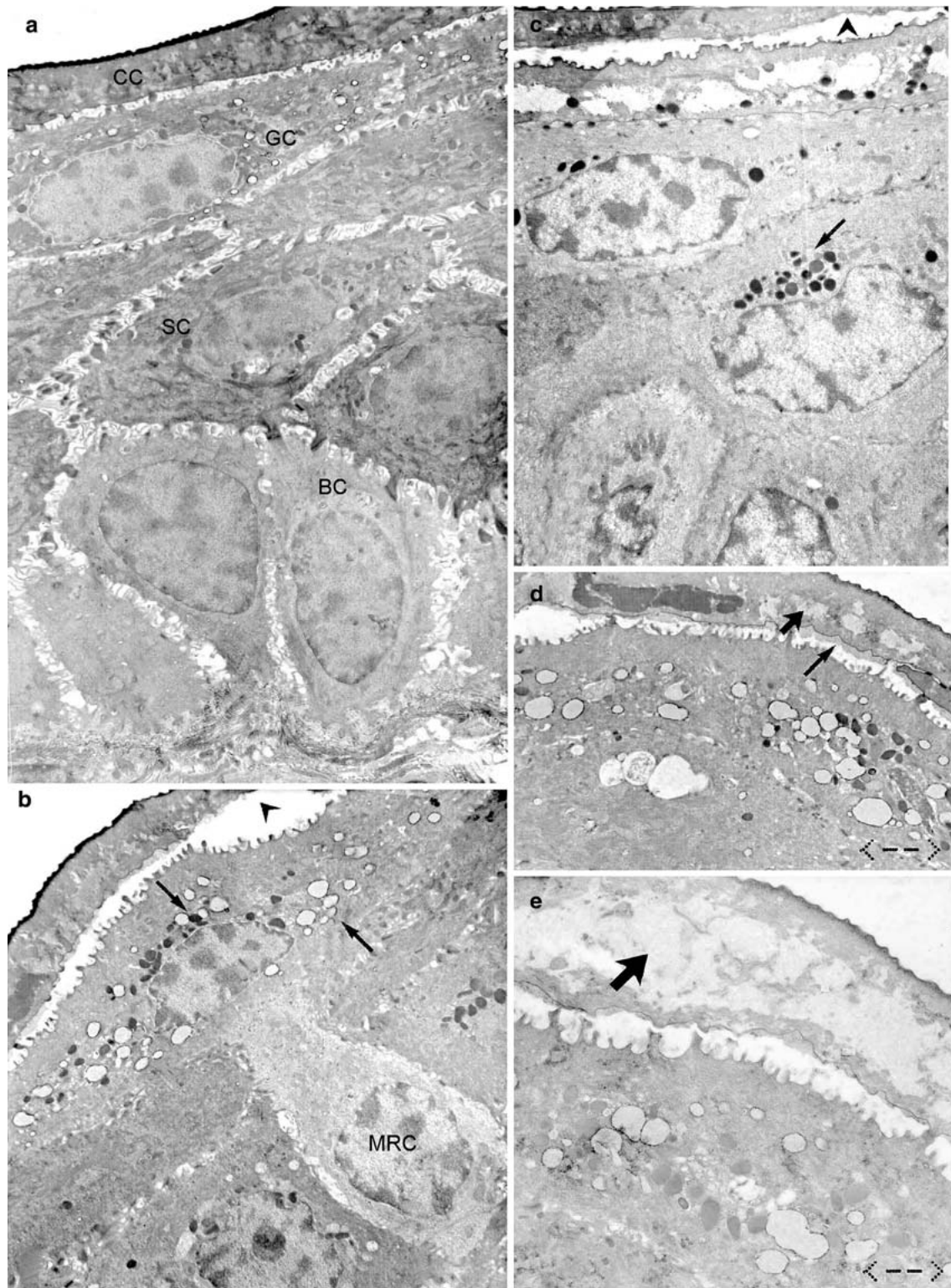
Fig. 1. Electron micrographs of epidermis. (**a**) Control frog epidermis showing basal cells with relatively abundant cytoplasms and few tonofilaments inside along with intermediate layer cells having an increased number of mucous granules and tonofilaments (arrows) inside (CC-horny cells; GC-granulous cells; SC-spinous cells; BC-basal cells). (**b** through **e**) Epidermis of polluted animals. (**b** and **c**) Granulous cells containing numerous granules and vesicles (arrows); note the presence of a dilated interstice beneath the horny coat (arrowheads) and an MRC in (**b**). (**d** and **e**) Superficial cells showing pale amorphous areas inside the cytoplasm (thick arrows); note deposits of amorphous material beneath the horny coat (arrow). Scale bar for **a**, **b**, **c**, **d** = 2.3 μm; scale bar for **e** = 1.7 μm
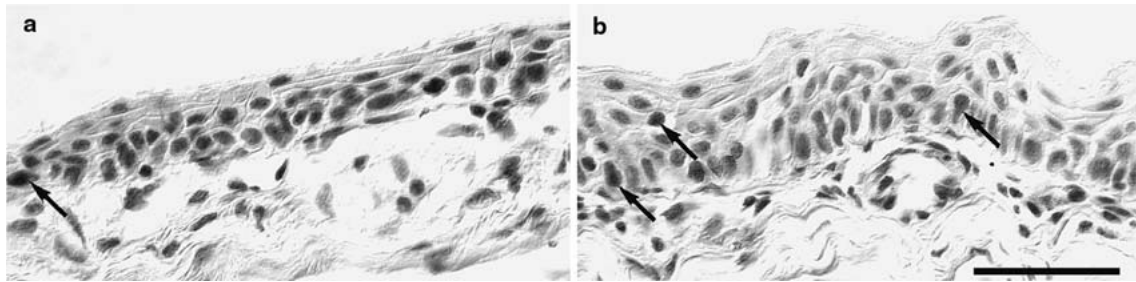
Fig. 2. TUNEL assay. Specimens of control (**a**) show occasional positive nuclei (arrow); in polluted frog epidermis (**b**), a few labelled nuclei are located mainly in the basal layer (arrows). Scale bar = 50 µm
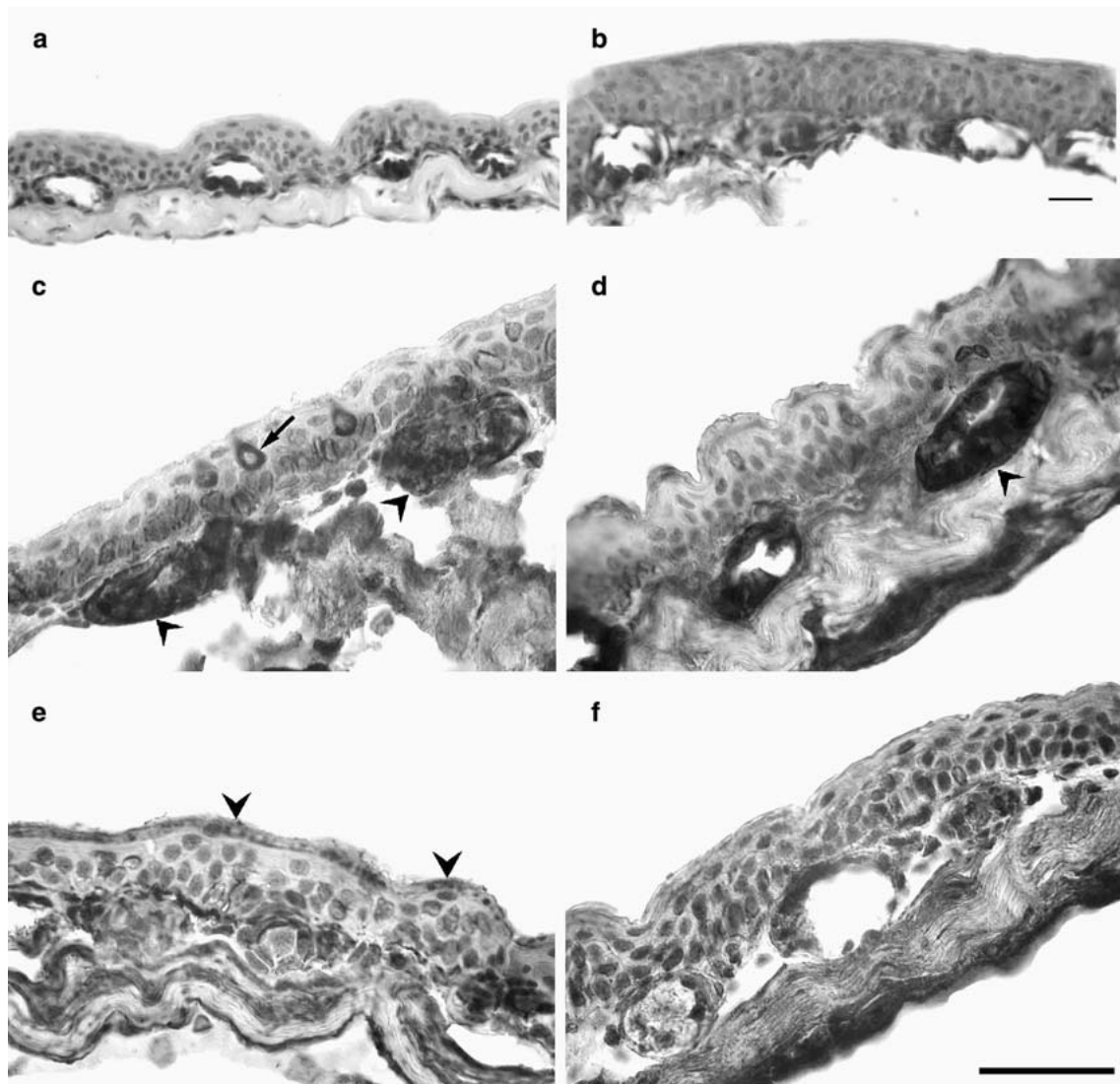
Fig. 3. PAS staining (**a** and **b**) beside involving secretory cells in mucous glands. In the control epidermis, the reactivity is light from basal to intermediate layers (**a**), while it is intense in almost all layers of polluted samples (**b**). AE1 immunostaining. (**c**) Moderate to strong immunopositivity is noted in the epidermal basal layer and in MRC (arrow) of control frogs. (**d**) In polluted samples, moderate immunopositivity labels basal, corneus, and MRC cells. Also, mucocytes in subepidermal glands show strong immunoreactivity (arrowheads in **c** and **d**). AE2 immunostaining. (**e**) Intense immunodeposits are observable in the corneus layer of the control samples (arrowheads). (**f**) Weak immunopositivity is detected in the horny coat of the polluted frogs. Scale bar = 50 µm
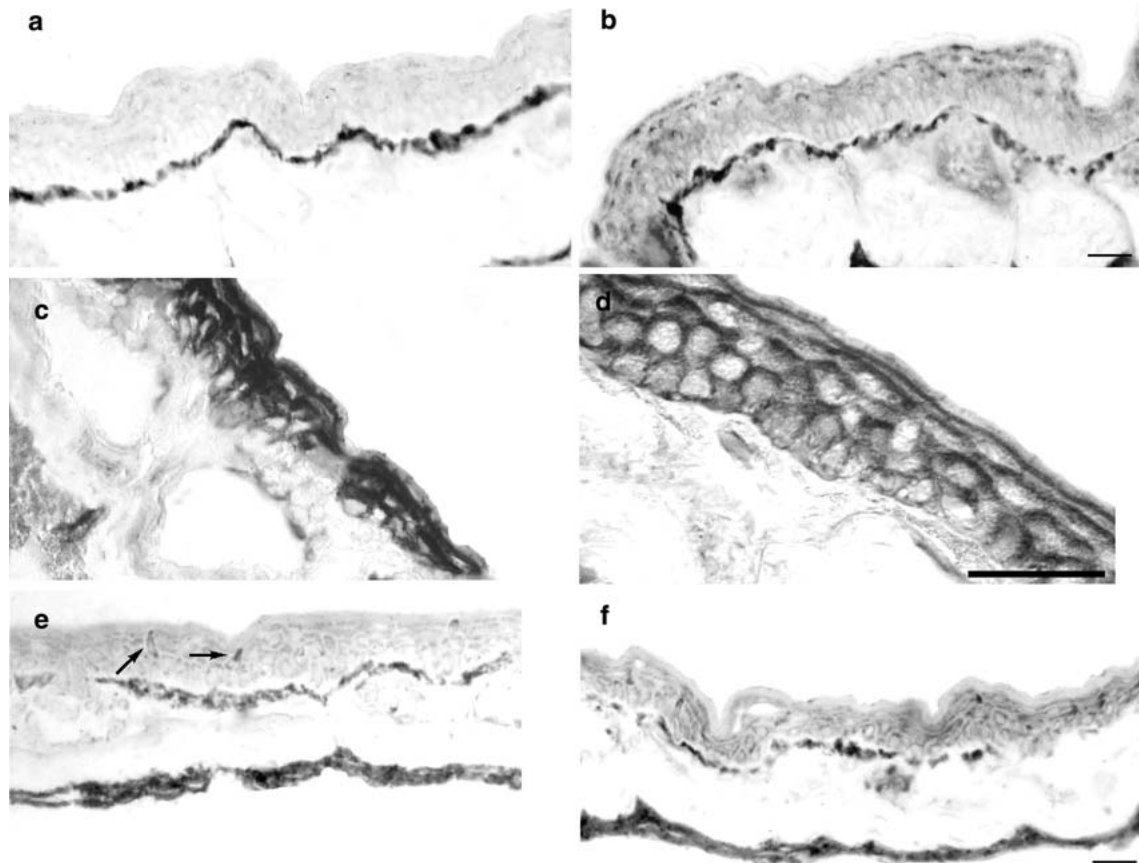
Table 3. Evaluation of immunohistochemical expression of cytokeratins in the frog epidermis[a]

Cytokeratins	Control frogs				Polluted frogs			
	HL	IL	BL	MRCs	CL	IL	BL	MRCs
AE1	−	−	++	+++	+	−	++	++
AE2	++	−	−	−	+	−	−	−
AE3	++	+	+	+	+	+	+	+

BL = basal layer.

HL = horny layer.

IL = intermediate layers.

[a]+++ Intense staining; ++ moderate staining; + wake staining; − negative.

Fig. 4. Comparison of the enzyme histochemistry of the frog epidermis between control (**a, c,** and **e**) and polluted (**b, d,** and **f**) animals. Activity of AcPase is mainly localized in the upper regions of cells in intermediate strata and in the layer beneath the horny coat in both control (**a**) and polluted (**b**) samples, although stronger reaction products are visible in the polluted ones. The staining pattern of AlkPase activity increases from the uppermost to the outer layers, except for the horny coat, in both groups of animals. The reactivity is strong in control frog epidermis (**c**) and weak to moderate in polluted frog (**d**). NOS/NADPHd activity is detected in both keratinocytes and MRCs (arrows), with an increased reactivity in polluted samples (**f**) compared with controls (**e**). Scale bar = 50 μm

CAT staining gave almost-negative responses in the epidermis of control animals, whereas the upper epidermal layers of the polluted samples showed moderate positivity. A few cells lying between basal layer and dermis, likely interstitial mononuclear cells, were intensely reactive for CAT in polluted samples (Figs. 5c and 5d).

Moderate to dense SDH reaction product labelled the MRCs mainly in the apical pole in the epidermis of all specimens.

The reaction gave similar results, and there was no noticeable difference in staining patterns between control and polluted samples. The amounts of the reaction products were variable among cells in either group (data not shown).

The reactions for both esterases were positive in controls, labelling the cells of the upper epidermis layers with a graded intensity (Figs. 5e and 5f). In animals from polluted sites, the amounts of the product of the reaction for ANAE was
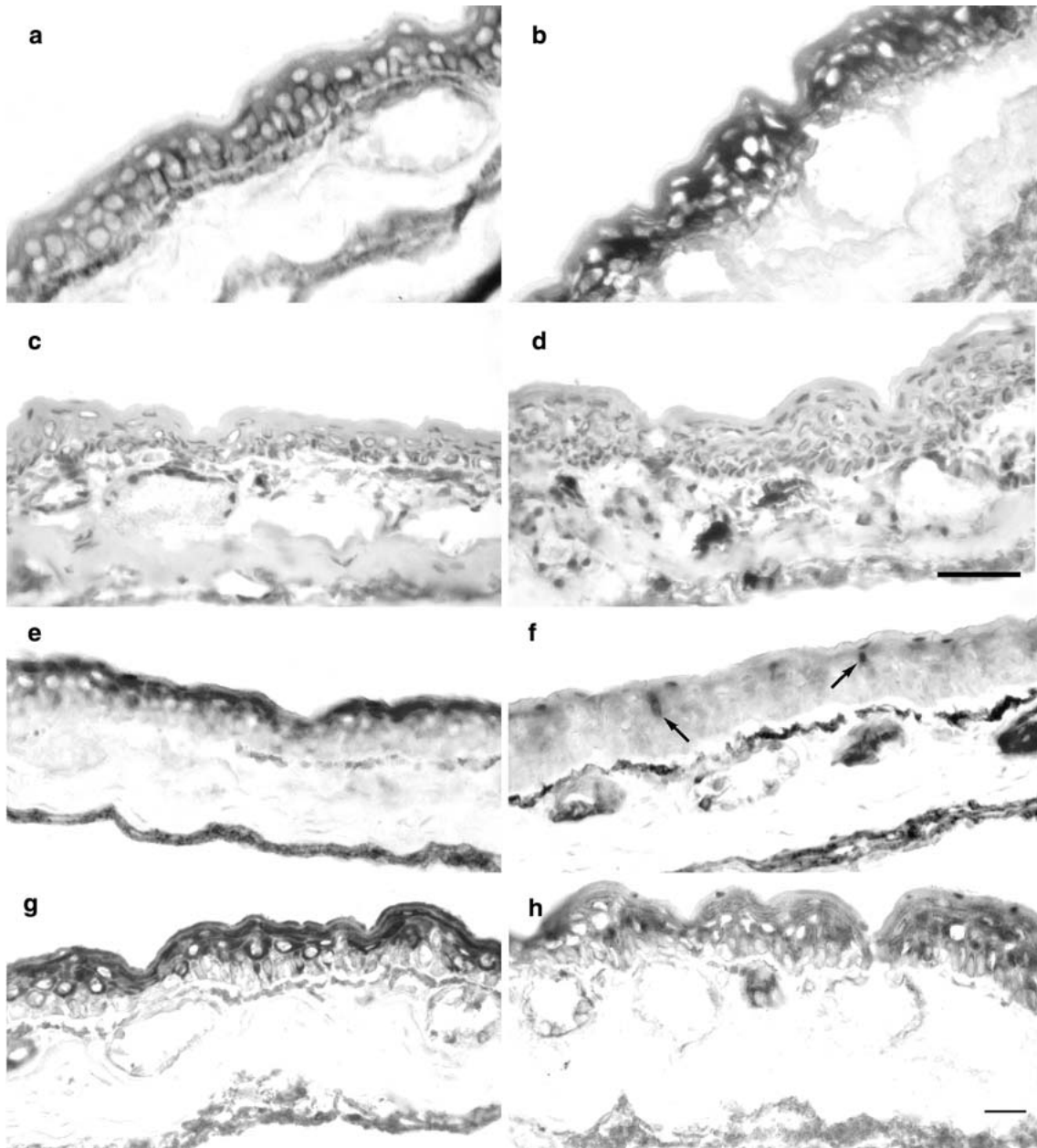
Fig. 5. Comparison of the enzyme histochemistry of the frog epidermis in control (**a**, **c**, **e**, and **g**) and polluted (**b**, **d**, **f**, and **h**) animals. G6PDH activity appears moderate in the basal and intermediate layers of control samples (**a**), whereas strong G6PDH activity is observable in the intermediate layers of polluted frogs (**b**). CAT activity is negligible in the epidermis of controls (**c**), but in polluted samples, keratinocytes of the upper layers show a moderate activity; note a few positive cells between basal layer and dermis (**d**). ANAE and ANBE activities are intense in the upper epidermis layers of control samples (**e** and **g**); in polluted animals, ANAE staining is mainly detected in the MRCs (arrows in **f**), whereas light ANBE staining involves keratinocytes in all of the epidermal layers except the horny one (**h**). Scale bar = 50 μm

remarkably high in MRCs, whereas decreased staining of keratinocytes was noticed in all of the epidermal layers after both ANAE and ANBE staining (Figs. 5g and 5h).

The results of enzyme histochemistry are summarized in Table 4.

ROS expression in the epidermis of both control and polluted animals was negligible or scant. Samples from the polluted sites showed patterns of ROS expression in some cells, possibly interstitial cells, lying between the epidermis and dermis (data not shown).

Discussion

In the current investigation, we analyzed some morphofunctional aspects of the green frog epidermis with the aim of highlighting possible defense mechanisms against environmental contamination. Previous chemical analyses conducted on tadpoles (Fenoglio *et al.* 2005) and present investigations performed on both sediments and adult frogs confirmed a high level of contamination in the site we supposed to be chemically polluted. In sediments from the polluted environment, we

Table 4. Evaluation of enzyme activities in the epidermis[a]

Enzyme activity	Control frogs		Polluted frogs	
	Keratinocytes	MRCs	Keratinocytes	MRCs
AcPase	+/++	−	++/+++	−
AlkPase	+++	−	++	−
NOS/NADPH	+	++	+/++	+++
G6PDH	++	−	++/+++	−
CAT	±	−	+	−
SDH	−	+++	−	++/+++
ANAE	++	++	+	++
ANBE	++	−	+	−

[a]+++ Intense staining; ++ moderate staining; + wake staining; − negative.

found concentrations of cadmium and mercury higher than critical levels, and, in some cases, their concentrations exceeded the established hazard limits in sediments (Mac Donald *et al.* 2000). Interestingly, the tissue concentrations of contaminants fitted those in sediments, except for lead. In samples of adult frogs collected in the polluted site, the values of cadmium, mercury, and lead were higher than those reported in literature for species of the genus *Rana* (Baudo 1976; Terhivuo *et al.* 1984; Pauli *et al.* 2000).

The heptachlor epoxide level in sediments was lower than the critical concentration in both sites (Mac Donald *et al.* 2000). There were no reference values about the other organic compounds we considered.

Heptachlor and heptachlor epoxide occurred in tissues from both control and polluted samples in concentrations resembling those found in other species of *Rana* (Pauli *et al.* 2000). No data were available on endosulfan background values in the literature.

In general, it is conceivable that the concentrations of tissue contaminants were the result of middle- or long-term bioaccumulation from more or less persistent water and sediment pollution. As a consequence of environmental contamination, we evidenced some consistent changes in the structural features and enzyme activities in the skin of polluted frogs compared with controls.

Remarkable morphologic modifications were detected in polluted frog skin, though none of the samples displayed signs of degeneration. However, TUNEL-positive cells probably represent damaged keratinocytes, which are removed by way of apoptotic cell death.

Compared with controls, most superficial cells of polluted specimens showed in their cytoplasms a larger amount of amorphous and electron transparent material associated with bundles of tonofilaments. Yet, amorphous material was also detected in the subcorneal space, whereas cells in intermediate epidermal layers often contained mucous products and vesicles of different sizes within the cytoplasm. In the same samples—and particularly in the superficial cells—we observed intense PAS positivity and AcPase activity, consistent with morphologic traits in the epidermis of contaminated frogs.

It is worthy of note that in larval stages, epidermal development involves mucogenic activity, and the first background material required to clump keratin filaments is mucous in nature. The ontogenic transition from larval to adult epidermis is characterized by the disappearance of large mucous granules, whereas dense, round, mucous-like deposits were found

among keratin filaments (Fox 1986; Alibardi 2001, 2003). In the present investigation, the detection of large and electron-transparent deposits of amorphous material (probably mucous) in most horny layers of polluted samples suggests that these specimens are involved in decreased maturation of the superficial cell layer.

Interestingly, differences in keratin immunostaining distribution along the epidermal layers were evidenced in the two groups of frogs considered polluted and unpolluted. The superficial cells of polluted animals expressed higher AE1 immunopositivity than AE2 compared with controls. Furthermore, relevant AE1 immunostaining was also detected in MRCs and in mucous gland cells of both groups.

Studies conducted by Alibardi (2001, 2002) in adult skin of different amphibian species have demonstrated AE1 immunopositivity mainly in basal layers, AE2 immunopositivity in the external layers, and AE3 throughout epidermis, thus indicating AE2 as a specific marker for keratinization. In fact, AE2 immunostaining indicates the presence of 63-kDa keratin during terminal differentiation of anuran skin keratinocytes (Nishikawa *et al.* 1992). Moreover, AE2-positive keratins are typical of stratified and keratinized layers in the epidermis of amniotes (O' Guin *et al.* l987; Alibardi 2001).

Generally, keratins are thought to provide structural integrity to cells to counteract mainly physical stressors on tissues. Studies performed on keratinocyte cells lines, characteristic of pathologic conditions in humans (*i.e.*, epidermolysis bullosa) and defective for keratins CK5 and CK14, have suggested that some keratins play a role in preserving tissue structure during osmotic stress (D'Alessandro *et al.* 2002).

Taking into account the relevant role of the frog epidermis in ion and water transport (Lindemann and Voute 1976), it is likely that the changes we found in both morphologic features and cytokeratin expression in epidermis of polluted frogs probably affect the barrier role and the transport function of this epithelium.

In this respect, the decreased activity of AlkPase, an enzyme involved in transmembrane transport processes, found in polluted animals may be significant. Noteworthy are previous investigations (Suwalsky *et al.* 2000) showing that mercuric compounds affect sodium transport in isolated skin of toad.

Nitric oxide (NO), produced by NOS, can be involved in regulative processes of skin physiology. In mammals, all three NOS isoforms, *i.e.*, neuronal (nNOS), inducible (iNOS), and endothelial (eNOS), have been detected in keratinocytes.

Notably, iNOS expression has been found in a number of inflammatory skin conditions (see Cals-Grierson and Ormerod [2004] for a review). In the present investigation, we found an increase in NOS/NADPH expression in keratinocytes and in MRCs of the polluted specimens compared with controls. In amphibian skin, Nilsson *et al.* (2000) described the paracrine role of NO in modulating pigment granules distribution within melanophores. However, Cals-Grierson and Ormerod illustrated in their review (2004) the numerous biological functions of the NO-signalling molecule in normal and pathologic conditions of human skin, *i.e.*, response to UV radiation, melanogenesis, antimicrobial effects, the maintenance of this skin barrier function, and wound healing. It has also been reported that NO seems to inhibit the keratinization processes in human skin (Rossi *et al.* 2000), thus contrasting the barrier function of skin. We cannot therefore exclude a possible correlation of the NOS/NADPH activity observed in frog skin, as well as its variations in the staining positivity observed in polluted samples, with the adaptive processes of the skin. Possibly these processes are consistent with the degree of epidermal cells keratinization and width of the subcorneal space. Additional functional changes taking place in the epidermis of polluted frogs were suggested by variations in other enzyme activities. We observed differences between control and polluted specimens involving G6PDH and CAT activities. Both are considered antioxidant enzymes; the former produces NADPH, the major reducing compound present in the cytoplasm, and the latter degrades H_2O_2 into water and molecular O. The concomitant increase in polluted animals of both enzyme activities may be indicative of the ability of frog skin to counteract oxidative stress through an enzymatic action, as happens in mammal skin (Shindo *et al.* 1994; Muramatsu *et al.* 2005). In particular, the increase of G6PDH activity in the skin of polluted frogs indicates an adaptive response to contaminant exposure as observed in a previous investigation performed on livers of the same samples (Fenoglio *et al.* 2005). The present data, together with those reported in the literature (Pandolfi *et al.* 1995; Izawa *et al.* 1998; Winzer *et al.* 2001) seem to confirm the involvement of this enzyme in counteracting toxic and oxidative stress.

Moreover, observations on the activity of both antioxidant enzymes may be related to the patterns of ROS expression in the polluted samples that exhibited no noticeable differences compared with control frogs. Thus, an increase in antioxidant enzyme activity may be effective in preventing the formation of dangerous free radicals in animals living in polluted areas.

In contrast, in the present investigation, esterase activities (ANAE and ANBE) were observed to have generally diminished in polluted animals but ANAE in MRCs. Notably, esterases have proven to be good markers of the toxic effects of environmental contaminants on different organisms (Venturino *et al.* 2003; Maier 1978; Cachot *et al.* 1994). Numerous studies have shown that nonspecific esterases are zinvolved in the susceptibility or resistance of organisms (plants, protists, invertebrates, and vertebrates) to organophosphate pesticides, depending on the organisms and esterase isoforms. Actually, these enzymes seem to interact with insecticides in one of two possible ways: insecticides could inhibit them or be degraded by esterases (Feng 1997; Barbier *et al.* 2000 for a review).

Our results are indicative of an inhibiting effect of contaminants on epidermal esterases, except for the ANAE expressed in MRCs, probably due to a different susceptibility to contaminants of these cells or to the presence of different ANAE isoforms. In this regard, Barbier *et al.* (2000) have studied ANAE in two species of dinoflagellates, *Prorocentrum micans* and *Crypthecodinium cohnii,* showing different morphofunctional traits, photosynthetic and not photosynthetic, respectively. They found different sensitivity of ANAE to parathion in the two protests and suggested that this depended on specific cell characteristics.

On the whole, the present results point to two main adaptive changes in the epidermis of the frog *R. esculenta* in response to environmental contamination: (1) the increase of some antioxidant enzyme activities and (2) the decrease of keratinization. From a functional point of view, these studies suggest that, although the frog epidermis is sensitive to contamination, it is equipped with efficient defense mechanisms and seems to behave more as an active chemical barrier than as a passive physical shield when exposed to contaminants.

The current study has also evidenced for the first time the ANAE and NOS/NADPH activities in the MRCs, suggesting additional roles for these epidermal cells characteristic in amphibians, in addition to those demonstrated in the past, *i.e.*, acid–base regulation (Guardabassi *et al.* 1972), active ion transport (Lodi 1971; Zaccone *et al.* 1986; Larsen *et al.* 1992), and secretion process during sloughing (Lavker 1971; Budtz and Larsen 1975; Masoni and Romeu 1979). In fact, they seem to actively cooperate with the epidermal principal cells in the defensive responses to environmental stressors.

References

Alibardi L (2001) Keratinization in the epidermis of amphibians and the lungfish: Comparison with amniote keratinization. Tissue Cell 33:439–449

Alibardi L (2002) Immunocytochemical localization of keratins, associated proteins and uptake of histidine in the epidermis of fish and amphibians. Acta Histochem 104:297–310

Alibardi L (2003) Adaptation to the land: The skin of reptiles in comparison to that of the amphibians and endotherm amniotes. J Exp Zool 15:l2–41

Amstrup J, Froslev J, Willumsen NJ, Mobierg N, Jespersen A, Larsen EH (2001) Expression of cystic fibrosis transmembrane conductance regulator in the skin of the toad, *Bufo bufo,* and possible role for Cl^- transport across the heterocellular epithelium. Comp Biochem Physiol A 130:539–550

Bader M (1980) A systematic approach to standard addition methods in instrumental analysis. Chem Educ 57:703–775

Barbier M, Prevot P, Soyer-Gobillard MO (2000) Esterases in marine dinoflagellates and resistance to the organophosphate insecticide parathion. Int Microbiol 3:117–123

Barni S, Bernocchi G, Gerzeli G (1987) Nuclear changes and morphology of the epidermis in the hibernating frog. Tissue Cell 19(6):817–825

Baudo R (1976) Heavy metals concentrations (Cr, Cu, Mn and Pb) in tadpoles and adults of *Rana esculenta*. L Mem Ist Ital Idrobiol 33:325–344

Budtz PE, Larsen LO (1975) Structure of the toad epidermis during the moulting cycle. II. Electron microscopic observations on *Bufo bufo* (L.). Cell Tissue Res 159:459–483

Burstone MS (1962) Enzyme histochemistry. Academic, New York

Cachot J, Romana LA, Galgani F (1994) In vivo esterase activity in protoplasts as a bioassay of environmental quality. Aquat Bot 48:297–312

Cals-Grierson MM, Ormerod AD (2004) Nitric oxide function in the skin. Nitric Oxide 10:179–193

Castell-Rodriguez AE, Sampedro-Carrillo EA, Herrera-Henriquez MA, Rondan-Zarate A (2001) Non-specific esterase-positive dendritic cells in epithielia of the frog *Rana pipiens*. Histochem J 33:311–316

D'Alessandro M, Russel D, Morley SM, Davies AM, Lane B (2002) Keratin mutations of epidermolysis bullosa simplex alter the kinetics of stress response to osmotic shock. J Cell Sci 115:4341–4351

De Piceis Polver P, Fenoglio C, Rapuzzi G, Gerzeli G, Barni S (1988) Potassium-dependent p-nitrophenyl phosphatase and adenylate cyclase activity in *Rana esculenta* skin during natural hibernation and active life: A cytochemical study. Arch Biol 99:183–195

Ehrenfeld J, Masoni A, Garcia-Romeau F (1976) Mitochondria-rich cells of frog skin in transport mechanism: morphological and kinetic studies on transepithelial excretion of methylene blue. Am J Physiol 231:120–126

Ehrenfeld J, Klein U (1997) The key role of the H$^+$ V-ATPase in acid-base balance and Na$^+$ transport process in frog skin. J Exp Biol 200:247–256

Ellison TR, Mathisen PM, Miller L (1985) Developmental changes in keratin patterns during epidermal maturation. Dev Biol 112:329–337

Fasola M, Movalli PA, Gandini C (1998) Heavy metal, organochlorine pesticide, and PCB residues in eggs and feathers of herons breeding in northern Italy. Arch Environ Contam Toxicol 34:87–93

Feng PCC, Ruff TG, Rangwala SH, Rao SR (1997) Engineering plant resistance to thiazopyr herbicide via expression of a novel esterase deactivation enzyme. Pestic Biochem Physiol 59:89–103

Fenoglio C, Necchi D, Civallero M, Ceroni M, Nano R (1997) Cytochemical demonstration of nitric oxide synthase and 5'nucleotidase in human glioblastoma. Anticancer Res 17:2507–2512

Fenoglio C, Boncompagni E, Fasola M, Gandini C, Comizzoli S, Milanesi G, Barni S (2005) Effects of environmental pollution on the liver parenchymal cells and Kupffer-melanomacrophagic cells of the frog *Rana esculenta*. Ecotoxicol Environ Safe 60:259–268

Ferrari L, Salibian A (1999) Effect of cadmium on the epidermic structure of *Bufo arenarum* tadpoles: Influence of the chemical composition of the incubation media. Arch Physiol Biochem 107:91–96

Fox H (1986) The skin of amphibia: Epidermis. In: Bereiter-Hahn J, Matoltsy AG, Richards KS (eds). The integument. volume 2. Vertebrates. Springer, New York, pp 472–498

Fox H (1992) Figures of Eberth in the amphibian larval epidermis. J Morphol 212:87–97

Guitart R, Puig P, Gómez-Catalán J (1993) Requirement for a standardized nomenclature criterion for PCBs: computer-assisted assignment of correct congener denomination and numbering. Chemos 27:1451–1459

Fuchs E, Marchuk D (1983) Type I and type II keratins have evolved from lower eukaryotes to form the epidermal intermediate filaments in mammalian skin. Proc Natl Acad Sci U S A 80:5857–5861

Guardabassi A, Campantico E, Oliviero M (1972) Effect of environmental changes on the skin and pituitary gland of *Xenopus laevis* Daudin. Specimens treated and untreated with prolactin. Monit Zool Ital 6:129–146

Higgy KE, Burns GF, Hayhoe FJC (1977) Discrimination of B, T and null lymphocytes by esterase cytochemistry. Scand J Haematol 18:99–106

Hoffman W, Franz JW (1984) Amino acid sequence of the carboxy-terminal part of an acidic type I cytokeratin of molecular weight 51000 from *Xenopus laevis* epidermis as predicted from cDNA sequence. EMBO J 3:1301–1306

Hoffman W, Franz JW, Franke WW (1985) Amino acid sequence microheterogeneities of basic (Type II) cytokeratins of *Xenopus laevis* epidermis and evolutionary conservativity of helical and non-helical domains. J Mol Biol 184:713–724

Izutsu Y, Kaiho M, Yoshizato K (1993) Different distribution of epidermal basal cells in the anuran larval skin correlates with the skin's region-specific fate at metamorphosis. J Exp Zool 267:605–615

Izawa S, Maeda K, Miki T, Mano J, Inoue Y, Kimura A (1998) Importance of glucose-6-phosphate dehydrogenase in the adaptive response to hydrogen peroxide in *Saccharomyces cerevisiae*. Biochem J 330:811–817

Johnson MS, Vodela JK, Reddy G, Holladay SD (2000) Fate and the biochemical effects of 2,4,6-trinitrotoluene exposure to tiger salamanders (*Ambystoma tigrinum*). Ecotoxicol Environ Safe 46:186–191

Kerver ED, Vogels IM, Bosch KS, Vreeling-Sinderalova H, Van den Munckof RJ, Frederiks WM (1997) In situ detection of spontaneous superoxide anion and singlet oxygen production by mitochondria in rat liver and small intestine. Histochem J 29:229–237

Kohen R (1999) Skin antioxidants: Their role in aging and in oxidative stress—New approaches for their evaluation. Biomed Pharmacother 53:181–192

Larsen EH, Willumsen NJ, Christoffersen BC (1992) Role of proton pump of mitochondria-rich cells for active transport of chloride ions in toad skin epithelium. J Physiol 450:203–216

Lavker RM (1971) Fine structure of clear cells in frog epidermis. Tissue Cell 3:567–578

Lindeman B, Voûte C (1976) Structure and function of the epidermis. In: Llinas RR, Precht H (eds). Frog neurobiology. Springer Verlag, New York, pp 169–210

Lodi G (1971) Histoenzymologic characterization of the flask cells in the skin of the crested newt under normal and experimental conditions. Atti Accad Si Torino Cl Sci Fis Mat Natur 105:561–571

Loyda Z, Gossrau R, Schiebler TH (1979) Enzyme histochemistry. A laboratory manual. Springer Verlag, New York

Mac Donald DD, Ingersoll CG, Berger TA (2000) Development and evaluation of consensus based sediment quality guidelines for freshwater ecosystems. Arch Environ Contam Toxicol 39:20–31

Maier R (1978) Blei und seine Auswirkung auf Aktivität und multiple Formen der Alpha-Naphtyl-Esterase in bleichteten und verdunkelten pflanzen. Ber Dtsch Bot Ges 91:39–350

Malvin GM, Hlastala MP (1989) Effects of environmental O$_2$ on blood flow and diffusing capacity in amphibian skin. Respir Physiol 76:229–241

Marchetti R (1991) Quadro complessivo delle condizioni delle acque del fiume Po negli anni '90 e tendenze evolutive. Atti Conv. La qualità delle acque del fiume Po negli anni '90, Ferrara, 18–20 Aprile 1990. Quad IRSA 92:16.1–16.26

Masoni A, Garcia Romeu F (1979) Moulting in *Rana esculenta:* Development of mitochondira-rich cells, morphological changes of the epithelium and sodium transport. Cell Tissue Res 197:23–38

Mateo R, Gámez A, Guitart R (1998) Organochlorine residues in hunted wild mallards in the Ebro delta, Spain. Bull Environ Contam Toxicol 60:134–141

Mateo R, Saavedra D, Guitart R (1999) Reintroduction of the otter (*Lutra lutra*) into Catalan rivers, Spain: Assessing organochlorine residue exposure through diet. Bull Environ Contam Toxicol 63:248–255

McGadey J (1970) A tetrazolium method for non-specific alkaline phosphatase. Histochemie 23:180–184

Muramatsu S, Suga Y, Mizuno Y, Hasegawa T, Matsuba S, Hashimoto Y (2005) Differentiation-specific localization of catalase and hydrogen peroxide, and their alterations in rat skin exposed to ultraviolet B rays. J Dermatol Sci 37:151–158

Nakos G, Gossrau R (1994) When NADPH diaphorase (NADPHd) works in the presence of formaldehyde, the enzyme appears to visualize selectively cells with constitutive nitric oxide synthase (NOS). Acta Histochem 96:335–343

Nilsson HM, Karlsson AM, Loitto VM, Svensson SP, Sundqvist T (2000) Nitric oxide modulates intracellular translocation of pigment organelles in *Xenopus laevis* melanophores. Cell Motil Cytoskeleton 47:209–218

Nishikawa A, Shimizu-Nishikawa K, Miller L (1992) Spatial, temporal, and hormonal regulation of epidermal keratin expression during development of the frog *Xenopus laevis*. Dev Biol 151:145–153

O'Guin MW, Galvin S, Schermer A, Sun TT (1987) Patterns of keratin expression define distinct pathways of epithelial development and differentiation. In: Moscona AA, Monroy A (eds). Current topics in developmental biololgy. Volume 22. Academic, New York, pp 97–123

Pandolfi PP, Sonati F, Rivi R, Mason P, Grosveld F, Luzzatto L (1995) Targeted disruption of the housekeeping gene encoding glucose-6-phosphate dehydrogenase (G6PD): G6PD is dispensable for pentose synthesis but essential for defense against oxidative stress. EMBO J 14:5209–5215

Pauli BD, Perrault JA, Money SL (2000) RATL: A database of reptile and amphibian toxicology literature. Technical Report Series No. 357. Hull, Quebec, Canada, Headquarters, Canadian Wildlife Service

Pearse AGE (1972) Histochemistry, theoretical and applied volume Churchill Livingstone, London, pp 344–349

Robinson H, Heintzelman M (1987) Morphology of ventral epidermis of *Rana catesbeiana* during metamorphosis. Anat Rec 217:305–317

Rossi A, Catani MV, Candi E, Bernassola F, Puddu P, Melino G (2000) Nitric oxide inhibits cornified envelope formation in human keratinocytes by inactivating transglutaminases and activating protein. J Invest Dermatol 115:731–739

Shindo Y, Wirt E, Han D, Epstein W, Packer L (1994) Enzymic and nonenzymic antioxidants in epidermis and dermis of human skin. J Invest Dermatol 102:122–124

Spies I (1997) Immunolocation of mitochondria-rich cells in the epidermis of the common toad, *Bufo bufo* L. Comp Biochem Physiol B 118:285–291

Suzuki K, Sato K, Katsu K, Hayashita H, Kristenses DB, Yoshizato K (2001) Novel *Rana* keratin genes and their expression during larval to adult epidermal conversion in bullfrog tadpoles. Differentiation 68:44–54

Suwalsky M, Norris B, Cardenas H (2000) Mercuric chloride (HgCl$_2$) and methyl mercury (CH$_3$HgCl) block sodium transport in the isolated skin of the toad *Pleurodema thaul*. Bull Environ Contam Toxicol 65:794–802

Suwalsky M, Ungerer B, Villena F, Norris B, Cardenas H, Zatta P (2001) Effects of AlCl$_3$ on toad skin, human erythrocytes, and model cell membranes. Brain Res Bull 55:205–210

Suwalsky M, Schneider C, Norris B, Cardenas H (2004) Effects of Pb^{2+} ions on Na$^+$ transport in the isolated skin of the toad *Pleurodema thaul*. Biometals 17:655–668

Terhivuo JM, Ldenius P, Nuorteva P, Tulisalo E (1984) Mercury content of common frogs (*Rana temporaria* L.) and common toads (*Bufo bufo* L.) collected in southern Finland. Ann Zool Fennici 21:4l–44

Vanatta JC, Frazier W (1989) Histological changes in the skin of *Rana pipiens* produced by metabolic alkalosis. Tissue Cell 21:219–227

Van Noorden CJF, Jonges GN (1987) Quantification of the histochemical reaction for alkaline phosphatase activity using the indoxyl-tetranitro BT method. Histochem J 19:94–102

Van Noorden CJF, Frederiks WM (1992) Enzyme histochemistry. A laboratory manual of current methods. Oxford University Press, Oxford, UK

Venturino A, Rosenbaum E, Caballero de Castro A, Anguiano OA, Gauna L, Fonovich de Schroeder, et al. (2003) Biomarkers of effect in toads and frogs. Biomarkers 8:167–186

Winzer K, Becker W, Van Noorden CJF, Kohler A (2001) Quantitative cytochemical analysis of glucose-6-phosphate dehydrogenase activity in living isolated hepatocytes of European flounder for rapid analysis of xenobiotic effects. J Histochem Cytochem 49:1025–1032

Zaccone G, Fasulo S, Lo Cascio P, Licata A (1986) Enzyme cytochemical and immunocytochemical studies of flask cells in the amphibian epidermis. Histochemistry 84:5–9